

Atomistic Band Gap Engineering in Donor–Acceptor Polymers

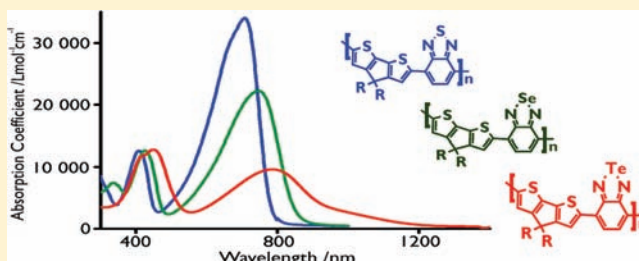
Gregory L. Gibson, Theresa M. McCormick, and Dwight S. Seferos*

Lash Miller Chemical Laboratories, Department of Chemistry, University of Toronto, 80 St. George Street, Toronto, Ontario M5S 3H6, Canada

S Supporting Information

ABSTRACT: We have synthesized a series of cyclopentadithiophene–benzochalcogenodiazole donor–acceptor (D–A) copolymers, wherein a single atom in the benzochalcogenodiazole unit is varied from sulfur to selenium to tellurium, which allows us to explicitly study sulfur to selenium to tellurium substitution in D–A copolymers for the first time. The synthesis of S- and Se-containing polymers is straightforward; however, Te-containing polymers must be prepared by postpolymerization single atom substitution. All of the polymers have the representative dual-band optical absorption profile, consisting of both a low- and high-energy optical transition.

Optical spectroscopy reveals that heavy atom substitution leads to a red-shift in the low-energy transition, while the high-energy band remains relatively constant in energy. The red-shift in the low-energy transition leads to optical band gap values of 1.59, 1.46, and 1.06 eV for the S-, Se-, and Te-containing polymers, respectively. Additionally, the strength of the low-energy band decreases, while the high-energy band remains constant. These trends cannot be explained by the present D and A theory where optical properties are governed exclusively by the strength of D and A units. A series of optical spectroscopy experiments, solvatochromism studies, density functional theory (DFT) calculations, and time-dependent DFT calculations are used to understand these trends. The red-shift in low-energy absorption is likely due to both a decrease in ionization potential and an increase in bond length and decrease in acceptor aromaticity. The loss of intensity of the low-energy band is likely the result of a loss of electronegativity and the acceptor unit's ability to separate charge. Overall, in addition to the established theory that difference in electron density of the D and A units controls the band gap, single atom substitution at key positions can be used to control the band gap of D–A copolymers.



INTRODUCTION

In 1992 Wynberg and co-workers introduced the concept of the donor–acceptor (D–A) approach to conjugated polymer design.^{1,2} In the intervening years, this has become a widely used method for preparing conjugated polymers with narrow band gaps.^{3–18} The approach involves synthesizing a polymer with a delocalized π -electron system that comprises alternating electron-rich (donor) and electron-deficient (acceptor) repeat units. The combination of high-lying HOMO levels (residing on the donor units) and low-lying LUMO levels (residing on the acceptor units) results in an overall narrow band gap for the polymer. The band gap can be narrowed or widened on the basis of the choice of donor and acceptor units, or more specifically, the difference in electron density between the donor and acceptor units along the polymer backbone. The tunable nature of the D–A polymer approach is highly desirable and has resulted in extensive exploration of these materials with respect to light-harvesting and light-emitting applications.^{19–22} Indeed, this approach has been used to create a variety of chromophores that span the color spectrum.^{23,24}

In the vein of tuning and controlling the band gap of D–A polymers, researchers have focused on exchanging donor and acceptor units for stronger or weaker ones,^{6,15,25,26} or altering the donor to acceptor ratio within the polymer structure.^{23,27,28} One of the hallmarks of D–A polymers is a dual-band optical

absorption spectrum. This dual-band is responsible for broad absorption characteristics. The origin of this dual-band, however, is not fully understood.¹⁸ Two separate transitions, that arise as the result of either (1) charge transfer between the donor and acceptor units along with a π – π^* transition that is centered on the donor unit,^{15,29} or (2) a reorganization of molecular orbitals to produce easily accessible low- and high-lying energy levels spread across both donor and acceptor units,^{30–32} are considered to give rise to the dual-band absorption spectrum.

One of the challenges with determining structure–property relationships in D–A polymers, and hence the origin of the dual-band absorption, is that functional groups are used to change and control electronic properties. A far more direct means to understand structure–property relationships in D–A polymers would be to carry out a study whereby a single atom is systematically varied in either the donor or acceptor moiety and properties are determined. To the best of our knowledge, however, no such study has been reported in the literature.

Herein, we present a study in which the heteroatom of the acceptor moiety of the fused-thiophene-containing D–A polymer, poly(cyclopentadithiophene)benzothiadiazole

Received: September 21, 2011

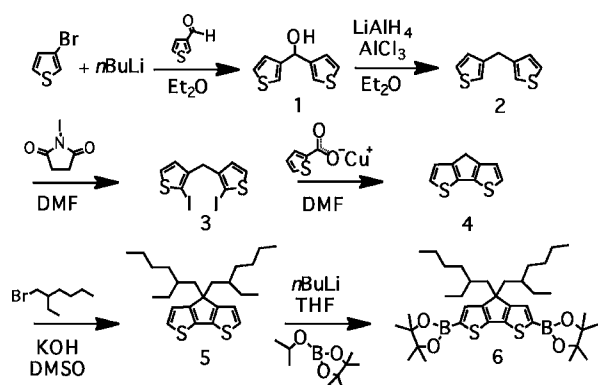
Published: November 30, 2011

(PCPDTBT), is systematically varied from sulfur to selenium to tellurium. Using optical measurements as well as density functional theory (DFT) calculations, we illustrate several surprising trends in D–A behavior upon single atom substitution in the acceptor unit, which cannot be explained simply by the strength of D and A units. These trends are then used to explain the dependence of optical properties on the identity of the heteroatom in the acceptor structure. More broadly, we are able to use these model systems to draw specific conclusions with regard to the origin of the dual-band optical absorption in general classes of D–A polymers.

RESULTS

Synthesis. In order to study the effect of single atom substitution on the PCPDTBT system, we carried out a synthesis to prepare three chalcogen analogs of this polymer. PCPDTBT is an important material, however, it can be very challenging to prepare. The methodology for the synthesis of PCPDTBT begins with the synthesis of the fused-thiophene donor monomer (Scheme 1). Several syntheses of this core

Scheme 1. Synthesis of fused-thiophene monomer building block



molecule have been published.^{33,34} Most routes involve alkylation of the bridge carbon followed by functionalization at the distal ends with appropriate groups for condensation polymerization. In this work, we report a modified approach that reduces the number of steps and the time required for purification.

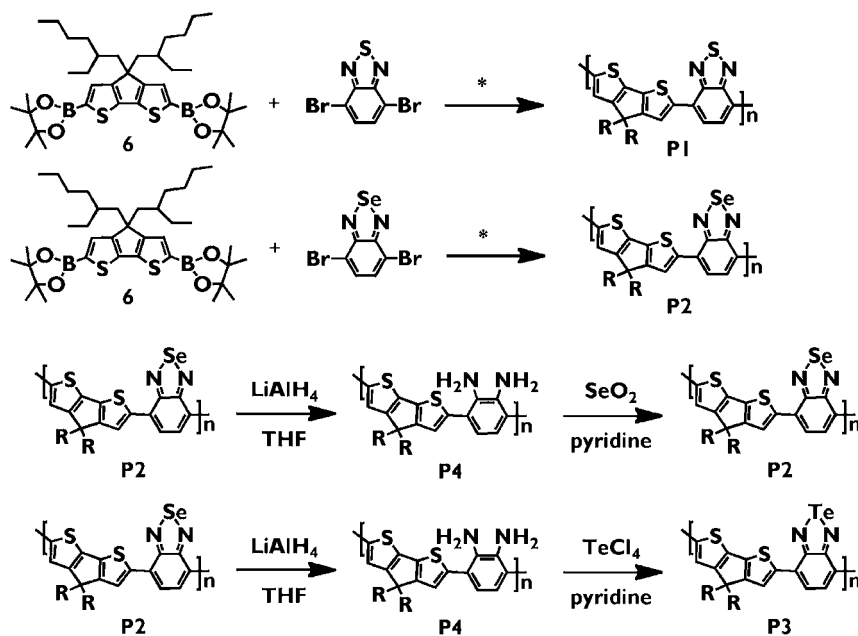
The first step in the synthesis of the fused-thiophene donor monomer involves treating 3-bromothiophene with *n*-butyllithium to form the 3-thienolithium species, and subsequent treatment with thiophene-3-carboxaldehyde to join two thiophene rings by a bridge carbon at their respective 3-positions. The aldehyde is reduced to an alcohol in the process (1). Further reduction at the bridge carbon with LiAlH₄ and AlCl₃ affords 2 in 75% yield. The next step, forming the bond that fuses the thiophene rings and forms the planar core, presents the greatest synthetic challenge. This sequence has previously been carried out by dibromination followed by a copper-catalyzed Ullmann coupling reaction.³⁴ In our case, we chose a unique copper reagent, copper(I)thiophene carboxylate,³⁵ which allows conventional heating and eliminates the need for activated copper, which can be difficult to use. Because copper(I)thiophene carboxylate works best with iodinated aromatic substrates, *N*-iodosuccinimide was used to first install iodine at the 2 and 2' positions of 2, affording 3, which is the precursor to the Ullmann coupling step. The optimized conditions for the Ullmann coupling step, as

determined from ¹H NMR spectroscopy, involve treating the iodinated precursor 3 with 5 equivalents of copper(I)thiophene carboxylate in *N,N'*-dimethylformamide at 70 °C for 48 h. Purification by column chromatography using silica as the stationary phase furnished the fused-thiophene, 4, in 60% yield.

With the monomer core in hand, we next carried out a method to install alkyl chains at the bridge position of the fused-thiophene system, which are essential for the solubility of the final polymeric material. Based upon our previous experiences, solubility is reduced for heavy chalcogen analogs of conjugated polymers.^{36–38} As such, we chose 2-(ethyl)hexyl side chains because these branched structures prevent aggregation and improve solubility in common organic solvents.¹² As well, branched side chains disrupt the crystallinity of the final material,³⁹ which may allow us to investigate the effects of single atom substitution on supramolecular interactions. Accordingly, the bridge carbon in 4 was deprotonated by treatment with potassium hydroxide, followed by treatment with 1-bromo-2-ethylhexane in dimethyl sulfoxide to afford 5 in 58% yield. To afford bis-boronic ester 6 that is suitable for Suzuki-coupling-polymerization, 5 was initially brominated at the 5 and 5' positions prior to treatment with *n*-butyllithium and 2-isopropoxy-4,4,5,5-tetramethyl-1,3,2-dioxaborolane. The Suzuki reagent 6 was found to be unstable when exposed to silica gel, however, making purification of the final monomer difficult. To circumvent these problems, 5 was purified on silica gel and reacted directly with *n*-butyllithium followed by addition of 2-isopropoxy-4,4,5,5-tetramethyl-1,3,2-dioxaborolane, to produce 6, which was sufficiently pure after workup to be used in subsequent polymerization reactions.

The acceptor molecules containing S, Se, and Te were synthesized by following literature procedures.^{40,41} Suzuki cross-coupling condensation polymerization was used to copolymerize the S and the Se acceptors, individually, with the fused-thiophene donor. This led to 56% and 51% yields of S- and Se-containing polymers (P1 and P2) respectively, after extraction to remove catalyst and low molecular weight polymers (Scheme 2). Copolymerization with the Te acceptor (structurally analogous to S and Se acceptors in Scheme 2) proved more difficult than the lighter analogs, even under mild Pd-catalyzed conditions.³⁸ As such, we conducted variable temperature absorption experiments to determine the stability of this monomer under typical polymerization conditions (Figure S1, Supporting Information). These studies revealed that this acceptor decomposes above 50 °C. Having determined that heat could not be used during condensation polymerization of this comonomer, several room temperature conditions were attempted for copolymerization; however, none of these conditions were successful at producing sufficiently high molecular weight polymer and thus we chose a unique approach to synthesize this macromolecule.

Specifically, we hypothesized that P3 could be obtained more readily by a postpolymerization modification of analogs P1 or P2. This methodology involves reducing either P1 or P2 to afford diamine P4, followed by reoxidation to form the Te-containing polymer. Experimentally, we determined that the Se-containing polymer P2 is quantitatively reduced with lithium aluminum hydride. Following that, reoxidation is accomplished by treatment with TeCl₄. The postpolymerization sequence was verified by NMR spectroscopy (Figure 1) and Se-elemental analysis (Table S1, Supporting Information). The ¹H NMR spectra of the aromatic region show clear shifting of the polymer proton resonances upon reduction of the Se-polymer

Scheme 2. Synthesis of D–A polymers P1–P3, Diamine Intermediate P4, and Re-oxidation of P4 back to P2^a

^a(*) Aliquat 336, K₂CO₃, Pd(PPh₃)₄, toluene, 80 °C, 72 h.

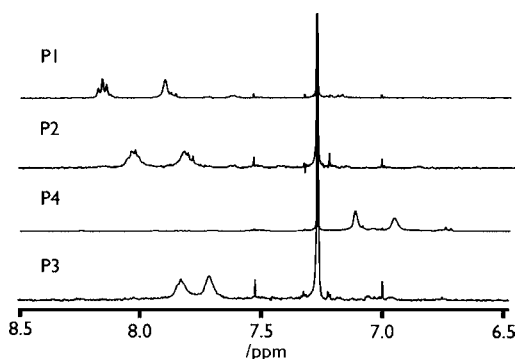


Figure 1. Aromatic region of the ¹H NMR spectra of polymers P1–P4 in CDCl₃ at 400 MHz.

to the diamine intermediate and subsequent reoxidation to the Te-polymer. Inductively coupled plasma atomic emission spectroscopy (ICP-AES) reveals that 97% of the Se content is removed upon conversion of P2 to P3 (Table S1, Supporting Information). Additional evidence for this transformation is available from absorption spectroscopy and is described in the next section. Finally, in control experiments, reoxidation of P4 with selenium oxide produced a polymer that was spectroscopically identical to P2, and lends further support to the success of the postpolymerization methodology (Figure S2 and S3, Supporting Information). Absorption spectra of two additional P2 samples, low ($M_n = 2300$ g/mol) and high ($M_n = 6000$ g/mol) molecular weight, were compared and found to be nearly identical (Figure S5, Supporting Information). Since P3 is prepared from P2 we conclude that the optical properties of the polymers are in the chain-length independent regime.

Optical Properties. In initial attempts to produce the Te polymer P3, the Te acceptor 4,7-dibromo-2,1,3-benzotelluradiazole was synthesized prior to conventional condensation polymerization. Thus, we began our spectroscopic studies with these three analogous acceptor molecules (S, Se, Te). Absorption properties were measured in solution to determine

the effect of heavy atom substitution (Figure 2). Here, we observe that the absorption maximum (λ_{max}) of these acceptors

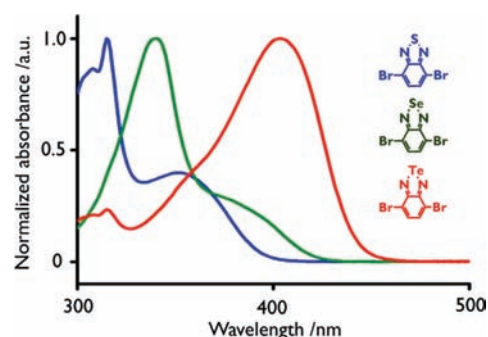


Figure 2. Absorption spectra of S, Se, Te acceptor molecules in DMSO.

shifts to longer wavelengths (lower energy) as one moves from S (315 nm) to Se (340 nm) to Te (404 nm). Not surprisingly, these spectra resemble those of other π -conjugated small molecules and do not possess the characteristic dual-band, which is indicative of a D–A system.¹⁸

The shift in optical absorption on moving from S to Se to Te is observed in the polymer absorption spectra (Figure 3). This trend is further illustrated by the energy of the optical band gap (measured from the absorption onset) of P1 (1.59 eV) when compared to P2 (1.46 eV) when compared to P3 (1.06 eV). The polymer spectra are more complicated than the small molecules and, specifically, the characteristic D–A dual-band is very apparent in polymers P1–P3. There are three general aspects of these spectra that are worth pointing out. First, the entire dual-band spectrum is shifted to a lower energy as heavier chalcogens are substituted into the acceptor molecule. Second, the low-energy band shifts by a greater extent than the high-energy band. Third, the absorption coefficient (based on the repeat unit molecular weight) of the low-energy band

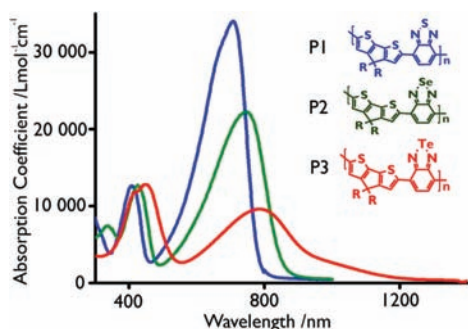


Figure 3. Absorption spectra in chloroform of group 16 D–A polymers, P1–P3.

decreases in intensity while the high-energy band remains constant upon moving down the group. Additionally, it is interesting that the diamine intermediate polymer P4 shows only a single absorption band that appears at approximately the same wavelength as the high-energy band in the D–A polymers (Figure S3, Supporting Information). Comparison with P1–P3 provides strong support that the dual-band only arises in D–A systems (the fused-thiophene and diamine units are energetically very similar, and both electron rich; see below).

It has been suggested in the literature that the low-energy band of the D–A dual absorption is due to an intramolecular charge transfer.^{15,29} This phenomenon should be evident in solvatochromic experiments. That is, the more polar excited state resulting from a charge transfer should be stabilized relative to the less polar ground state in a solvent of greater polarity. This excited state stability should result in a red-shift of the emission spectra of the polymers in more polar solvents. In order to identify a charge-transfer state, absorption and emission experiments were conducted on representative polymer P1 in solvents of increasing polarity (Figure 4).

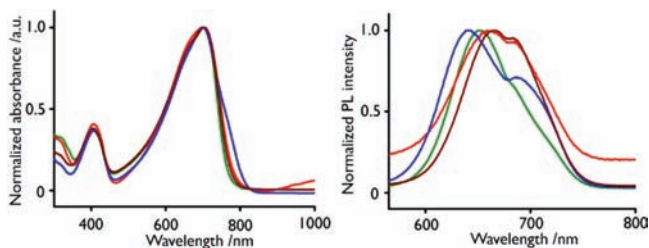


Figure 4. (Left) Absorption spectra of sulfur-containing P1 in cyclohexane (blue), toluene (green), chloroform (red) and tetrahydrofuran (wine). (Right) Emission spectra of sulfur-containing P1 in cyclohexane (blue), toluene (green), chloroform (red), and tetrahydrofuran (wine).

More specifically, the solvents tested, in order of increasing dielectric constant⁴² are cyclohexane ($\epsilon = 2.0$), toluene (2.4), chloroform (4.8), and THF (7.5). The absorption spectra of P1 in the four solvents remain the same, with a λ_{max} at approximately 700 nm. The emission spectra, however, are clearly shifted to lower energy, with λ_{em} transitioning from 743 to 752 nm to 758 to 766 nm upon moving from cyclohexane to toluene to chloroform to THF. The shift in the emission indicates that this optical excited state is, indeed, a charge transfer complex.

In order to understand the changing absorption coefficient in the dual-band spectrum on going from S to Se to Te, we investigated the effects of concentration on the absorption

spectrum of the representative polymer, P1 (Figure 5), which has the most intense low-energy transition. A solution of the

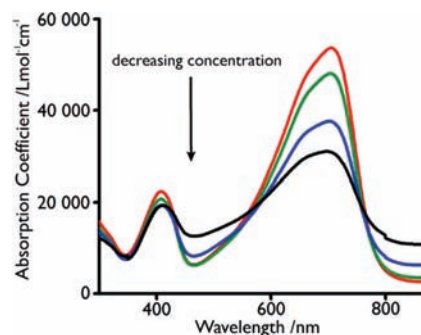


Figure 5. Absorption spectra of solutions of S-containing polymer P1 of decreasing concentration: 3.7×10^{-5} M (red), 1.9×10^{-5} M (green), 9.3×10^{-6} M (blue), 4.7×10^{-6} (black).

polymer was prepared and then diluted, and the absorption spectrum of each solution was obtained. Here we observe that, as the concentration of the solution decreases, the absorption coefficient of the high-energy band remains relatively constant while the low-energy charge transfer band decreases. This indicates an intermolecular charge transfer also contributes to this lower-energy absorption band; this is in addition to the well-established intramolecular charge transfer discussed earlier.

Density Functional Theory Calculations. To complement the optical characterization, the geometry, and electronic structure of small-molecule model dyads of the polymers P1–P4 (termed M1–M4), consisting of a single donor and acceptor pair with methyl groups in place of the 2-(ethyl)hexyl side chains, were calculated using DFT and time-dependent DFT (TD-DFT).⁴³ The coordinates of the optimized geometries (Supporting Information), the frontier orbitals involved in the lowest-energy singlet transitions (Figure 6), and the

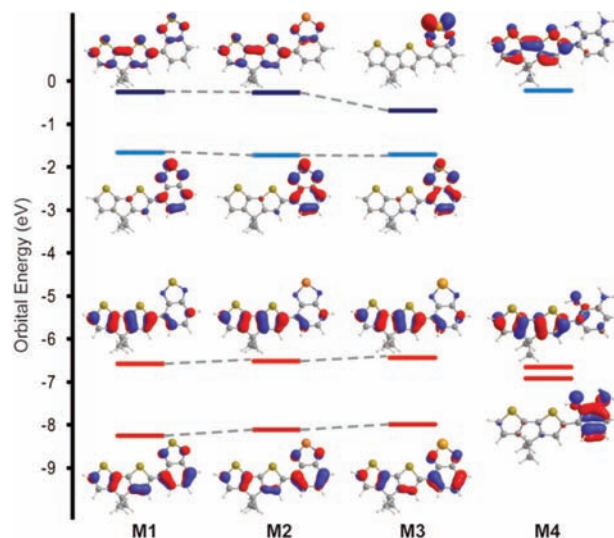


Figure 6. Frontier MO energy levels for model compounds M1–M4.

energies, orbitals, and oscillator strengths of the strongest transitions (Table 1) were calculated using the *Gaussian 09* program⁴⁴ at the CAM-B3LYP^{45–47} level of theory with the 6-31G(d) basis set for C, H, N, and S, and the LAN2DZ basis set⁴⁸ for Se and Te. We will first describe the frontier orbitals of

Table 1. TD-DFT Calculated Transition Data for Model Compounds M1–M4^a

	transition ^b	wavelength/nm (oscillator strength)	transition ^b	wavelength/nm (oscillator strength)
M1	H→L (+93%)	425 (0.48)	H→L+1(+86%)	311 (0.26)
M2	H→L (+92%)	445 (0.38)	H→L+1(+80%)	319 (0.31)
M3	H→L (+92%)	458 (0.33)	H→L+2(+42%); H-2→L(+33%)	327 (0.24)
			H-2→L(+46%); H→L +2(+27%)	316 (0.23)
M4	H→L (+91%)	314 (0.53)		

^aH = HOMO; L = LUMO. ^bCoefficient percentage of orbitals involved in the transition.

compounds M1–M3. All of these orbitals are very similar in electronic distribution. The HOMO resides on the fused-thiophene part of the molecule, while the LUMO is centered on the benzochalcogenodiazole acceptor part of the molecule. A slight destabilization of the HOMO and stabilization of the LUMO result from changing the heteroatom in the benzochalcogenodiazole from S to Se to Te, leading to an overall narrowing of the calculated HOMO–LUMO gap.

To further corroborate these trends TD-DFT calculations were carried out to model the ground-excited state transitions in these polymers (Figure 7). Both the high-energy and

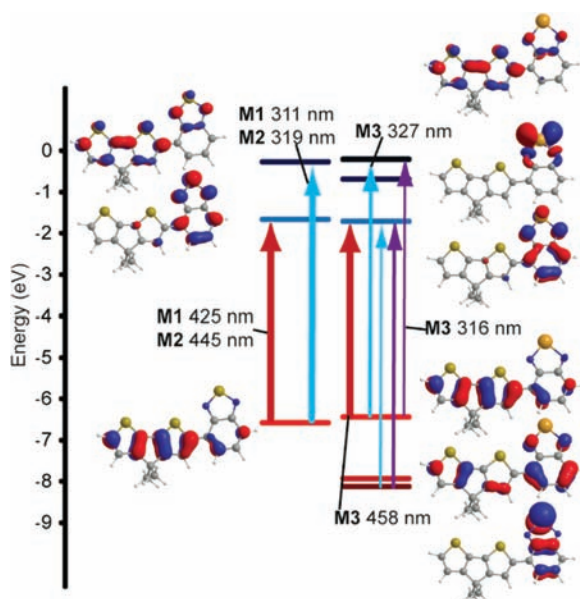


Figure 7. MO diagram of M1 on the left, the energy of the transitions calculated from TD-DFT are shown with the arrows illustrating the transition for both M1 and M2 as indicated. On the right the tellurium model compound M3 is shown with the arrows indicating electron transitions responsible for individual absorption bands. The thickness of each band is representative of the contribution of the orbitals to the transition.

low-energy bands are seen in the TD-DFT results (Table 1). For all three compounds, the lowest-energy singlet transition is a charge transfer from the HOMO on the fused-thiophene to the LUMO on the benzochalcogenodiazole. In changing the heteroatom from S to Se to Te for M1 to M3 this transition shifts from 425 to 445 nm to 448 nm, respectively. The oscillator strength of this transition also decreases as one moves

down the series. The high-energy band is the second intense singlet transition. This transition is HOMO to LUMO+1 and is based solely on the fused-thiophene, shifting from 311 to 319 nm for M1 and M2, respectively. In the case of M3, however, the high-energy band consists of two different transitions; both are a combination of HOMO to LUMO+2 and HOMO–2 to LUMO with wavelengths at 327 and 316 nm. The HOMO to LUMO+2 is centered on the fused-thiophene, and the HOMO–2 to LUMO is on the benzochalcogenodiazole. All high-energy bands also shift to a lower energy going down the period, although to a smaller extent than for the charge transfer transitions.

DISCUSSION

To our knowledge this is the first systematic study of S, Se, and Te atom substitution in D–A polymers. The results above shed significant light on the properties and fundamental mechanisms of D–A polymers in general, and this will be discussed in this section. The well-known polymer PCPDTBT (P1) was chosen as a starting point because of its demonstrated potential for use in organic electronic applications, particularly organic photovoltaic devices and field effect transistors.⁵ As well, it offered a convenient location where single atom substitution could be achieved using modular chemistry.

While the sulfur and selenium analogs (P1 and P2, respectively) were relatively straightforward to synthesize, the tellurium polymer (P3) proved much more difficult and required the use of a novel postpolymerization synthetic method. The dual-band absorption observed in the spectra of P1–P3 is typical of the D–A polymer architecture (Figure 3).¹⁸ In the case of P3 the presence of the dual-band absorption demonstrates that we have formed the heterocycle with tellurium postpolymerization, because only the reconstruction of an electron-deficient heterocycle would lead to this signature absorption spectrum.

The synthesis of the benzochalcogenodiazole small molecules, their subsequent polymerization, and the red-shifted absorption upon substituting S for Se for Te demonstrate that heavy atom substitution narrows the band gap of π -conjugated molecules in general. This stands in contrast to studies of the oxygen analog of P1. Optical properties change very little when substituting O in place of S.⁴⁹ In the case of the polymers reported here, the λ_{max} of the high-energy absorption band remains relatively constant on moving from S to Se to Te, shifting by only a few nanometers upon moving down group 16 (Figure 3). More remarkably, the λ_{max} of the low-energy band shifts significantly while its absorption coefficient decreases in intensity upon moving from S to Se to Te. These spectra, taken together with the electronic structure calculations, present at least three fundamental issues worth addressing in D–A polymers, namely: (a) the origin of the red-shift in the absorbance spectra, (b) the origin of the peak intensity changes on moving from S to Se to Te (high-energy band vs low-energy band), and most importantly (c) how the present study offers new insight into the D–A mechanism.

We will first discuss (a), the origin of the red-shift in optical properties for the series, P1–P3. One explanation is that the low-energy transition is due to a charge transfer from the fused-thiophene donor to the benzochalcogenodiazole acceptor. In all three polymers this transition is HOMO to LUMO, as supported by the molecular orbital calculations and optical measurements. The calculations indicate two possible contributions to the red-shift on going from P1 to P3. First, the

dipole moment of the ground state geometry is larger for **M1** (3.27 D) than for **M2** (2.82 D) and **M3** (1.55 D). This same trend is observed in the Mulliken charges on the chalcogenide atom, 0.57, 0.58, 0.79. The increased positive charge agrees well with the decrease in electronegativity upon going down the group. In agreement with previous theoretical calculations,⁵⁰ the lower ionization potential of the heavier atom leads to destabilization of the occupied bonding MO related to the LUMO. This stabilizes the LUMO of the polymer, thereby narrowing the band gap and producing a red-shift in the absorption spectrum as one moves from S to Se to Te. The incorporation of heavier atoms into polythiophene analogues, perhaps the most important class of conjugated polymers, has been fuelled by the observation that the HOMO of such polymers does not lie on the heavy atom, while the LUMO does, enabling a narrowing of the band gap by heavy-atom substitution.^{37,51,52}

A second reason for the greater shift in the low-energy transition is related to the degree of aromaticity found in the acceptor unit. A longer E–N bond length (where E = S, Se, or Te), produced upon single atom substitution, results in a disruption of conjugation within the benzene ring, as shown by the calculated bond lengths (Supporting Information). The degree of bond length alternation in the benzene ring increases in the order S to Se to Te, trending toward a decrease in aromaticity which affects the conjugation of the acceptor unit with the donor unit. This results in destabilization of the HOMO, stabilization of the LUMO, and an overall decrease in the band gap of the polymer. This is apparent not only in the decreasing calculated energy of the LUMO, as discussed above, which is concentrated on the benzochalcogenodiazole unit, but also by a destabilization of the HOMO energy level (Figure 6). A similar trend has been observed in thiophenes that have been modified to stabilize their quinoid state.^{53,54} We further note that the high-energy transition is centered entirely on the fused-thiophene and is, therefore, not expected to shift as strongly. This is consistent with the experimentally obtained absorption spectra of the polymers.

Now we will discuss (b), the origin of the peak intensity changes on moving from S to Se to Te. We observe that the absorption coefficient of the low-energy band decreases in intensity upon moving from S to Se to Te, while the high-energy band remains largely unaffected. This can be explained by the decreasing electronegativity of the heteroatom. In order to produce the low-energy absorption band, the acceptor unit must be electron-deficient enough to produce a charge separated state.¹⁸ As the electronegativity of the heteroatom decreases upon moving down group 16, the acceptor unit's ability to separate charge, as well as stabilize a charge-separated state, decreases. This reduction in ability to separate intramolecular charge leads to a decrease in the absorption coefficient of the low-energy band when moving from S to Se to Te.

Interestingly, a similar effect in the optical spectrum of the S-containing polymer **P1** was seen as the concentration of the polymer in solution was decreased (Figure 5). Given that only the intensity of low-energy charge transfer band is affected, this suggests that there may be an intermolecular charge transfer process at work as well as the intramolecular process previously described. It follows that as the concentration of polymer decreases, there are fewer opportunities for neighboring chains to interact, which would be necessary for intermolecular charge transfer to occur. This effect is more pronounced in **P1** as the

relatively high electronegativity of S favors charge transfer, both inter- and intramolecularly, to a greater extent than its heavier chalcogen analogs. This effect is not observed in Se-containing **P2** nor in Te-containing **P3** (Figure S4, Supporting Information). The absence of concentration effects and intermolecular charge transfer in **P2** and **P3** confirms our hypothesis that the greater electronegativity of S relative to that of Se and Te contributes to the relatively high intensity of the charge transfer band in the spectrum of **P1**.

Now we will discuss (c), how the present study offers insight into the D–A mechanism. Throughout the literature the notion that a charge transfer state causes the low-energy D–A transition is implied.¹⁷ Our DFT calculations predict a distinct HOMO and LUMO for the polymer repeat unit that has a charge transfer character. The majority contribution from the donor unit on the HOMO and majority contribution from the acceptor unit on the LUMO results in a significant shift of electron density as an electron is promoted from the ground to the excited state. The observation that the absorption coefficient of the low-energy transition does not shift as the S-containing polymer **P1** is exposed to solvents of increasing polarity is not surprising (Figure 4). It is expected that the solvents of greater polarity will stabilize the more polar excited state relative to the ground state. Thus, the red-shift observed in the PL spectrum supports that a charge-transfer excited state gives rise to the low-energy absorption.

The presence of a charge-transfer excited state highlights the difference between the two basic models that describe these D–A systems: (1) a low-lying charge transfer state results from the push–pull interaction of the donor and acceptor units and gives rise to the low-energy absorption band while a higher-energy transition centered on the donor repeat unit gives rise to the high-energy band in the absorption spectrum;^{15,17,29} and (2) the incorporation of donor and acceptor units results in a reorganization of molecular orbitals to give a HOMO and LUMO that do not produce a charge transfer and retain less character of either the donor or acceptor units.^{30–32} Our data support a model involving a D–A charge transfer state involving distinct MOs for the polymer.

It is also accepted throughout the literature that the source of the narrow band gap in D–A polymers is the difference in electron density between the donor and acceptor units.²³ As such, the absorption spectrum of a polymer can be shifted by either adding electron density to the polymer chain through the donor or removing electron density through the acceptor.¹⁷ Indeed, this has been shown to be the case in many systems, most recently through the addition of Lewis acids to the acceptor units.^{55,56} The observation that the band gap of PCPDTBT analogs narrows as heavier atoms are substituted at the heteroatom position is counterintuitive if the only factor governing the location of the absorption is the distribution of electron density in the main chain. If this were the case, one would expect the strength of the D–A interaction to decrease (resulting in a blue-shift of the absorption spectrum) as heavier atoms are substituted. This is because the decreasing electronegativity moving down the group should weaken the electron-withdrawing ability of the acceptor going from S to Se to Te. The opposite effect is observed, however, indicating that another process must be at work in these systems. Given that heavy atoms have demonstrated an ability to narrow the band gap of all-donor homopolymers, it seems reasonable to suggest that in the present case the lower ionization potential and loss of aromaticity overcome the loss of electron-withdrawing ability

of the acceptor on moving down group 16. These results indicate that the D–A polymer absorption is not governed solely by the electron-rich or electron-poor nature of the polymer chain. Further, this single atom substitution study introduces another method for controlling the absorption properties of D–A polymers through modular chemistry.

CONCLUSION

Three analogs of the well-known D–A polymer PCPDTBT have been synthesized, including a novel Te analog, which was prepared by a postpolymerization method involving reduction of the Se polymer, isolation of an amine intermediate, and reoxidation of the acceptor with tellurium(IV). By inserting Se and Te into the S position of 2,1,3-benzothiadiazole, the three polymers (P1–P3) allow for a systematic single atom substitution study. Optical spectroscopy reveals that the characteristic D–A dual-band is present in each of these polymers and that heavy atom substitution leads to a red-shift in the low-energy transition, while the high-energy band remains relatively constant in energy. The red-shift in the low-energy transition leads to optical band gap values of 1.59, 1.46, and 1.06 eV for the S-, Se-, and Te-containing polymers, respectively. In addition, the strength of the low-energy band decreases while the high-energy band remains relatively constant. A series of optical spectroscopy experiments, solvatochromism studies, and DFT calculations were used to understand the trends in the acquired spectra. The red-shift in the low-energy absorption is likely due to both a decrease in the ionization potential of the heavy atom and a decrease in aromaticity as one moves from S to Se to Te. The decreasing intensity of the low-energy band can be explained by the decrease in the ability of the acceptor to separate and stabilize charge, owing to the decreasing electronegativity of the chalcogen atom. These results imply that the substitution of heavy atoms into the acceptor can narrow the band gap of a D–A polymer. This was not predicted on the basis of the established theory that difference in electron density of the D and A units controls the band gap of D–A polymers. This study therefore introduces a new method for controlling the absorption properties of D–A polymers through modular chemistry.

EXPERIMENTAL SECTION

General Considerations. Unless stated otherwise, starting materials were purchased and used as received. 3-Bromothiophene, thiophene-3-carboxaldehyde, *n*-butyllithium (1.6 M in hexanes), and 2-bromo-2-ethylhexane were purchased from Acros Organics. Lithium aluminum hydride, aluminum(III)chloride, selenium(IV)oxide, and tellurium(IV)chloride were purchased from Alfa Aesar. *N*-Iodosuccinimide, 2-isopropoxy-4,4,5,5-tetramethyl-1,3,2-dioxaborolane, Aliquat 336, potassium carbonate, tetrakis-triphenylphosphinepalladium(0), and pyridine were purchased from Sigma-Aldrich. Potassium hydroxide and magnesium sulfate were purchased from Fisher Scientific. Copper(I)thiophene-2-carboxylate was purchased from Frontier Scientific. 4,7-Dibromo-2,1,3-benzothiadiazole and 4,7-dibromo-2,1,3-benzoselenadiazole were prepared according to published procedures.⁴⁰ Unless otherwise noted, all manipulations involving air- or water-sensitive reagents were performed under an atmosphere of dry nitrogen using conventional Schlenk techniques and glassware or in an Innovative Technologies glovebox. Solvents were sparged with nitrogen for 25 min and dried using an Innovative Technologies solvent purification system. In the case of P3 absorption experiments, chloroform was dried with calcium hydride and distilled under nitrogen before use. Deuterated chloroform was purchased from Cambridge Isotope Laboratories, and in the case of use with P3, was

dried with calcium hydride and distilled under nitrogen before use. *n*-Butyllithium was titrated before each use. NMR spectra were recorded on a Varian Mercury 400 spectrometer operating at 400 MHz for ¹H and 100 MHz for ¹³C. Chemical shifts are reported in ppm at ambient temperature. ¹H chemical shifts are referenced to the residual protonated chloroform peak at 7.26 ppm. Absorption spectra were recorded on a Varian Cary 5000 UV–vis–NIR spectrophotometer in either DMSO or chloroform, as noted, at ~0.01 mg/mL. Emission spectra were recorded on a Photon Technology International QuantaMaster 40-F NA spectrofluorometer in chloroform solution. Polymer molecular weights were determined with a Viscotek HT-GPC (1,2,4-trichlorobenzene, 140 °C) using Tosoh Bioscience LLC TSK-GEL GMH_{HR}-HT mixed-bed columns and narrow molecular weight distribution polystyrene standards. Masses were determined on a Waters GCT Premier ToF mass spectrometer (EI). ICP-AEOS samples were digested in aqua regia for four days at 70 °C before being filtered and diluted to 25 mL with deionized water. The samples were run on a Perkin-Elmer model Optima7300DV ICP AEOS, and selenium levels were quantified with National Institute of Standards and Technology standards. The detection limit was 0.1 μg selenium/mL.

Density Functional Theory Calculations. Geometry optimizations were performed for all model compounds (M1–M4) using the *Gaussian 09* program employing the Becke Three Parameter Hybrid Functionals Lee–Yang–Parr (B3LYP) including Handy and co-workers' long-range corrected version of B3LYP using the Coulombic-attenuating method (CAM-B3LYP). The standard 6-31G(d) basis set for C, H, N, S atoms, and LAN2DZ for Te and Se atoms was used. Starting geometries were generated using Gausview 05. A frequency calculation was performed on the optimized geometries to ensure a local minimum was found. From the optimized geometries time-dependent DFT (TD-DFT) calculations were carried out with the same basis sets used for geometry optimizations; the first 20 singlet and triplet states were calculated.

Synthesis and Characterization. *Di-3-thienylmethanol (1).* *n*-Butyllithium in hexanes (1.56 M, 14.5 mL, 22.2 mmol) was added dropwise to a solution of 3-bromothiophene (2.10 mL, 22.1 mmol) in dry diethyl ether (200 mL) at –78 °C. This mixture was allowed to stir at –78 °C for 30 min before thiophene-3-carboxaldehyde (1.97 mL, 22.3 mmol) was added dropwise. This mixture was stirred overnight and allowed to warm to room temperature. The mixture was washed with 0.1 M HCl (2 × 75 mL), 0.1 M NaOH (2 × 75 mL), and brine (2 × 75 mL). The organic layer was dried on magnesium sulfate, and the solvent was removed by rotary evaporation to produce a light-yellow oil that solidified on standing at room temperature (3.57 g, 82% crude). The crude product was taken to the next reaction without further purification. ¹H NMR (400 MHz, CDCl₃) δ: 7.28 (m, 2H), 7.18 (m, 2H), 7.02 (d of d, *J* = 8 Hz, 4 Hz, 2H), 5.90 (s, 1H), 2.82 (br s, 1H). ¹³C NMR (100 MHz, CDCl₃) δ: 145.0, 126.4, 126.3, 121.8, 69.1.

Di-3-thienylmethane (2). Aluminum chloride (8.76 g, 65.7 mmol) was added to a suspension of lithium aluminum hydride (2.45 g, 64.6 mmol) in dry diethyl ether (250 mL) at 0 °C over 10 min. Di-3-thienylmethanol was then added in portions over 10 min at 0 °C, and the mixture was heated to reflux for 5 h. The mixture was diluted with diethyl ether (150 mL) and quenched by adding 1 M HCl dropwise. Once the bubbling had subsided, the mixture was washed with 1 M HCl (150 mL), 1 M NaOH (150 mL), and brine (2 × 150 mL). All aqueous washings were separately extracted once with diethyl ether (75 mL), and all organic layers were combined and dried over magnesium sulfate, and the solvent was removed under vacuum to produce di-3-thienylmethane (7.08 g, 75%) as a yellow oil. ¹H NMR (400 MHz, CDCl₃) δ: 7.26 (d of d, *J* = 4 Hz, 2H), 6.94–6.98 (m, 4H), 4.01 (s, 2H). ¹³C NMR (100 MHz, CDCl₃) δ: 141.0, 128.4, 125.6, 121.1, 31.1. HR-MS 180.0067 calc. 180.0060 found.

Bis(2-iodothien-3-yl)methane (3). *N*-Iodosuccinimide (18.0 g, 80.0 mmol) was added to a solution of di-3-thienylmethane (7.03 g, 39.0 mmol) in dry DMF (250 mL) at 0 °C over 45 min. This mixture was stirred overnight with warming to room temperature. Following stirring, 0.1 M HCl (200 mL) was added, and the mixture was extracted with diethyl ether (3 × 150 mL). The ether layers were combined and washed with water (2 × 150 mL) and brine (2 × 150 mL)

and dried over magnesium sulfate, and the solvent was removed under vacuum to produce bis(2-iodo-3-yl)methane (12.3 g, 73%). ¹H NMR (400 MHz, CDCl₃) δ: 7.37 (d, *J* = 8 Hz, 2H), 6.67 (d, *J* = 8 Hz, 2H), 3.84 (s, 2H). ¹³C NMR (100 MHz, CDCl₃) δ: 144.2, 130.7, 128.3, 75.0, 35.0. HR-MS 431.8000 calc. 431.7999 found.

4*H*-Cyclopenta[2,1-*b*:3,4-*b'*]dithiophene (4). Dry DMF (250 mL) was added by cannula to bis(2-iodothien-3-yl)methane (14.9 g, 34.3 mmol). Copper(I)thiophene-2-carboxylate (32.7 g, 171 mmol) was added, and the mixture was stirred at 70 °C for 48 h. The mixture was diluted with ethyl acetate (40 mL) and filtered through a plug of silica. The ethyl acetate was removed from the mixture by rotary evaporation, and brine (200 mL) was added to the organic mixture. This brine/DMF mixture was extracted with hexanes (3 × 200 mL), and the combined organic layers were washed with brine (3 × 200 mL) and dried over magnesium sulfate, and the solvent was removed under vacuum to produce a brown oil which was purified by column chromatography on silica gel (pentane) to yield the title compound (3.64 g, 20.4 mmol, 60%) as a white solid. ¹H NMR (400 MHz, CDCl₃) δ: 7.19 (d, *J* = 4 Hz, 2H), 7.10 (d, *J* = 4 Hz, 2H), 3.56 (s, 2H). ¹³C NMR (100 MHz, CDCl₃) δ: 149.9, 138.9, 124.7, 123.2, 31.8. HR-MS 177.9911 calc. 177.9906 found.

4,4-Di(2-ethylhexyl)-4*H*-cyclopenta[2,1-*b*:3,4-*b'*]dithiophene (5). 1-Bromo-2-ethylhexane (7.30 mL, 40.8 mmol) was added to a solution of 4*H*-cyclopenta[2,1-*b*:3,4-*b'*]dithiophene (3.52 g, 19.8 mmol) in DMSO (80 mL), powdered KOH (3.65 g, 65.0 mmol), and KI (0.47 g, 2.8 mmol) under air. This mixture was allowed to stir at room temperature overnight and then poured out into water and extracted with diethyl ether (3 × 100 mL). The organic extracts were combined and dried over magnesium sulfate, and the solvent was removed under vacuum to give a brown oil which was purified by column chromatography on silica gel (hexane) to yield 4,4-di(2-ethylhexyl)-4*H*-cyclopenta[2,1-*b*:3,4-*b'*]dithiophene (4.58 g, 11.4 mmol, 58%) as a yellow oil. ¹H NMR (400 MHz, CDCl₃) δ: 7.10 (d, *J* = 4 Hz, 2H), 6.92 (m, 2H), 1.85 (m, 2H), 0.90 (m, 18H), 0.75 (t, *J* = 4 Hz, 2H), 0.58 (t, *J* = 4 Hz, 2H). ¹³C NMR (100 MHz, CDCl₃) δ: 157.8, 137.0, 124.1, 122.5, 53.4, 43.4, 35.2, 32.1, 29.0, 28.8, 23.0, 14.3, 10.8. HR-MS 402.2415 calc. 402.2405 found.

2,6-Bis(4,4,5,5-tetramethyl-1,3,2-dioxaboralan-2-yl)-4,4-di(2-ethylhexyl)-4*H*-cyclopenta[2,1-*b*:3,4-*b'*]dithiophene (6). A solution of 4,4-di(2-ethylhexyl)-4*H*-cyclopenta[2,1-*b*:3,4-*b'*]dithiophene (0.420 g, 1.04 mmol) in THF (15 mL) was cooled to -78 °C, and *n*-butyllithium in hexanes (1.6 M, 1.50 mL, 2.40 mmol) was added dropwise. This mixture was allowed to stir at -78 °C for one hour followed by warming to room temperature and stirring for a further 2 h. The mixture was subsequently cooled again to -78 °C, and 2-isopropoxy-4,4,5,5-tetramethyl-1,3,2-dioxaborolane (0.45 mL, 2.2 mmol) was added. This mixture was allowed to warm to room temperature with stirring overnight and subsequently poured into water (50 mL) and extracted with hexanes (3 × 50 mL). The organic layers were combined and washed with brine (3 × 50 mL) and dried on magnesium sulfate, and the solvent was removed under vacuum. The produced oil was further dried on a vacuum line for 24 h, producing a sticky orange product (622 mg, 0.941 mmol, 91%). ¹H NMR (400 MHz, CDCl₃) δ: 7.44 (t, 32H, *J* = 8 Hz), 1.84 (m, 4H), 1.34 (s, 24H), 0.96 (m, 18H), 0.73 (m, 6H), 0.58 (m, 6H). ¹³C NMR (100 MHz, CDCl₃) δ: 161.2, 144.3, 132.0, 84.1, 52.9, 43.4, 35.3, 34.1, 31.8, 28.5, 27.8, 25.0, 23.0, 14.3, 10.8. HR-MS (EI) *m/z*, calcd for C₃₇H₆₀B₂O₄S₂ (M⁺): 655.4210; found: 655.4197.

Poly[4,4-bis(2-ethylhexyl)cyclopenta[2,1-*b*:3,4-*b'*]dithiophene-2,6-diyl-*alt*-2,1,3-benzothiadiazole-4,7-diyl] (P1). In a nitrogen-filled glovebox, 2,6-bis(4,4,5,5-tetramethyl-1,3,2-dioxaboralan-2-yl)-4,4-di(2-ethylhexyl)-4*H*-cyclopenta[2,1-*b*:3,4-*b'*]dithiophene (0.133 g, 0.201 mmol), 1,2-dibromo-2,1,3-benzothiadiazole (0.060 g, 0.20 mmol), tetrakis-triphenylphosphinepalladium(0) (0.032 g, 0.028 mmol), and toluene (8 mL) were sealed inside a 50-mL reaction bomb. The reaction bomb was brought out of the glovebox and placed under nitrogen. Aliquot 336 (3 drops) and bubble-degassed aqueous potassium carbonate (2.0 M, 0.45 mL, 0.90 mmol) were added. The reaction bomb was sealed again, and the entire mixture was degassed by three freeze-pump-thaw cycles. The mixture was heated to 80 °C

under vacuum for 72 h before being poured into methanol (30 mL) and filtered through a Soxhlet thimble. The filtered solid was extracted with methanol, hexanes, and chloroform until each solvent in the extraction chamber was clear and colorless. The solvent was removed from the chloroform extract to yield the title polymer as a blue powder (0.022 g, 0.042 mmol, 56%). ¹H NMR (400 MHz, CDCl₃) δ: 8.14 (m, 2H), 7.88 (br s, 2H), 2.07 (br, 4H), 1.02 (br, 18H), 0.88 (br, 6H), 0.68 (br, 6H). GPC: *M_n* = 14 107 g/mol, *M_w* = 47 188 g/mol, PDI = 3.35.

Poly[4,4-bis(2-ethylhexyl)cyclopenta[2,1-*b*:3,4-*b'*]dithiophene-2,6-diyl-*alt*-2,1,3-benzoselenadiazole-4,7-diyl] (P2). This polymer was synthesized from 2,6-bis(4,4,5,5-tetramethyl-1,3,2-dioxaboralan-2-yl)-4,4-di(2-ethylhexyl)-4*H*-cyclopenta[2,1-*b*:3,4-*b'*]dithiophene (0.300 g, 0.454 mmol), 1,2-dibromo-2,1,3-benzoselenadiazole (0.154 g, 0.454 mmol), tetrakis-triphenylphosphinepalladium(0) (0.052 g, 0.045 mmol) in toluene (10 mL) in a manner that is analogous to P1 to yield P2 as a dark-green powder (0.062 g, 0.11 mmol, 51%). ¹H NMR (400 MHz, CDCl₃) δ: 8.02 (br m, 2H), 7.79 (br s, 2H), 2.05 (br s, 4H), 1.02 (br s, 16H), 0.88 (br s, 2H), 0.68 (br s, 12H). GPC: *M_n* = 5022 g/mol, *M_w* = 11 016 g/mol, PDI = 2.19.

Poly[4,4-bis(2-ethylhexyl)cyclopenta[2,1-*b*:3,4-*b'*]dithiophene-2,6-diyl-*alt*-2,3-diaminobenzo-1,4-diyl] (P4). Poly[4,4-bis(2-ethylhexyl)cyclopenta[2,1-*b*:3,4-*b'*]dithiophene-2,6-diyl-*alt*-2,1,3-benzoselenadiazole-4,7-diyl] (P2, 0.222 g, 0.380 mmol) was placed in a 100-mL Schlenk flask under nitrogen with dry THF (25 mL). Lithium aluminum hydride (0.150 g, 3.95 mmol) was added under nitrogen at 0 °C, and the resulting mixture was stirred at room temperature for 16 h. The mixture was poured into methanol (50 mL) and filtered through a Soxhlet thimble. The filtered solid was extracted with methanol, hexanes, and chloroform until each solvent in the extraction chamber was clear and colorless. The solvent was removed from the chloroform extract to yield the title polymer as a red solid (0.140 g, 0.275 mmol, 72%). ¹H NMR (400 MHz, CDCl₃) δ: 7.11 (s, 2H), 6.94 (s, 2H), 3.94 (br s, 4H), 1.96 (br s, 4H), 1.03 (br s, 18H), 0.79 (br s, 6H), 0.67 (br s, 6H).

Poly[4,4-bis(2-ethylhexyl)cyclopenta[2,1-*b*:3,4-*b'*]dithiophene-2,6-diyl-*alt*-2,1,3-benzotellurodiazole-4,7-diyl] (P3). Poly[4,4-bis(2-ethylhexyl)cyclopenta[2,1-*b*:3,4-*b'*]dithiophene-2,6-diyl-*alt*-2,3-diaminobenzo-4,7-diyl] (P4, 0.053 g, 0.11 mmol) was placed in a 10-mL Schlenk flask under nitrogen with dry pyridine (5 mL). Tellurium(IV)-chloride (0.036 g, 0.12 mmol) was added under nitrogen, and the resulting mixture was stirred at room temperature for 16 h. This mixture was poured out into dry methanol (15 mL), and the solid was collected by filtration, washed with dry methanol (30 mL), and dried under vacuum to give the title polymer as a dark-green solid (0.036 g, 0.057 mmol, 54%). ¹H NMR (400 MHz, CDCl₃) δ: 7.83 (s, 2H), 7.71 (s, 2H), 2.02 (br s, 4H), 1.03 (br s, 16H), 0.88 (br s, 2H), 0.69 (m, 12H).

Reoxidation of P4 to Poly[4,4-bis(2-ethylhexyl)cyclopenta[2,1-*b*:3,4-*b'*]dithiophene-2,6-diyl-*alt*-2,1,3-benzoselenadiazole-4,7-diyl] (P2). Poly[4,4-bis(2-ethylhexyl)cyclopenta[2,1-*b*:3,4-*b'*]dithiophene-2,6-diyl-*alt*-2,3-diaminobenzo-4,7-diyl] (P4, 0.023 g, 0.044 mmol) was placed in a 10-mL Schlenk flask under nitrogen with dry pyridine (5 mL). Selenium(IV)oxide (0.0060 g, 0.054 mmol) was added under nitrogen, and the resulting mixture was stirred at room temperature for 16 h. This mixture was poured into methanol (15 mL), and the solid was collected by filtration, washed with methanol (30 mL), and dried under vacuum to give the title polymer as a green solid (0.015 g, 0.026 mmol, 59%). GPC: *M_n* = 6363 g/mol, *M_w* = 11 747 g/mol, PDI = 1.85.

■ ASSOCIATED CONTENT

📄 Supporting Information

Additional absorption and NMR spectra as well as supplemental calculation data; complete ref 44. This material is available free of charge via the Internet at <http://pubs.acs.org>.

■ AUTHOR INFORMATION

Corresponding Author

dseferos@chem.utoronto.ca

■ ACKNOWLEDGMENTS

This work was supported by the University of Toronto, NSERC, the CFI, and the Ontario Research Fund. We are grateful to Professor Ignacio Vargas-Baca and Dr. Anthony Cozzolino (McMaster University) for assistance with the synthesis of 4, 7-dibromo-2,1,3-benzotelluradiazole. G.L.G. thanks the Xerox Research Centre of Canada for a Graduate Award.

■ REFERENCES

- (1) Havinga, E.; ten Hoeve, W.; Wynberg, H. *Polym. Bull.* **1992**, *29*, 119–126.
- (2) Havinga, E.; ten Hoeve, W.; Wynberg, H. *Synth. Met.* **1993**, *55*, 299–306.
- (3) Guo, X.; Watson, M. D. *Macromolecules* **2011**, *44*, 6711–6716.
- (4) Beaujuge, P.; Ellinger, S.; Reynolds, J. *Adv. Mater.* **2008**, *20*, 2772–2776.
- (5) Zhang, M.; Tsao, H. N.; Pisula, W.; Yang, C.; Mishra, A. K.; Müllen, K. *J. Am. Chem. Soc.* **2007**, *129*, 3472–3473.
- (6) Jayakannan, M.; Van Hal, P. A.; Janssen, R. A. J. *J. Polym. Sci. A: Polym. Chem.* **2001**, *40*, 251–261.
- (7) Zhou, E.; Nakamura, M.; Nishizawa, T.; Zhang, Y.; Wei, Q.; Tajima, K.; Yang, C.; Hashimoto, K. *Macromolecules* **2008**, *41*, 8302–8305.
- (8) Zhu, Z.; Waller, D.; Gaudiana, R.; Morana, M.; Mühlbacher, D.; Scharber, M.; Brabec, C. *Macromolecules* **2007**, *40*, 1981–1986.
- (9) Wang, E.; Wang, L.; Lan, L.; Luo, C.; Zhuang, W.; Peng, J.; Cao, Y. *Appl. Phys. Lett.* **2008**, *92*, 033307.
- (10) Wang, E.; Ma, Z.; Zhang, Z.; Vandewal, K.; Henriksson, P.; Inganäs, O.; Zhang, F.; Andersson, M. R. *J. Am. Chem. Soc.* **2011**, *133*, 14244–14247.
- (11) Burkhart, B.; Khlyabich, P.; Canak, T.; LaJoie, T.; Thompson, B. C. *Macromolecules* **2011**, *44*, 1242–1246.
- (12) Coffin, R. C.; Peet, J.; Rogers, J.; Bazan, G. C. *Nat. Chem.* **2009**, *1*, 657–661.
- (13) Bundgaard, E.; Krebs, F. C. *Macromolecules* **2006**, *39*, 2823–2831.
- (14) Guo, X.; Watson, M. *Macromolecules* **2011**.
- (15) Jenekhe, S. A.; Lu, L.; Alam, M. M. *Macromolecules* **2001**, *34*, 7315–7324.
- (16) Cheng, Y.-J.; Yang, S.-H.; Hsu, C.-S. *Chem. Rev.* **2009**, *109*, 5868–5923.
- (17) Beaujuge, P. M.; Reynolds, J. R. *Chem. Rev.* **2010**, *110*, 268–320.
- (18) Beaujuge, P. M.; Amb, C. M.; Reynolds, J. R. *Acc. Chem. Res.* **2010**, *43*, 1396–1407.
- (19) Öktem, G.; Balan, A.; Baran, D.; Toppare, L. *Chem. Commun.* **2011**, *47*, 3933.
- (20) Shen, C.; Rubin, Y.; Wudl, F. *Angew. Chem.* **2004**, *116*, 1524–1528.
- (21) Hains, A. W.; Liang, Z.; Woodhouse, M. A.; Gregg, B. A. *Chem. Rev.* **2010**, *110*, 6689–6735.
- (22) Beaujuge, P. M.; Subbiah, J.; Choudhury, K. R.; Ellinger, S.; McCarley, T. D.; So, F.; Reynolds, J. R. *Chem. Mater.* **2010**, *22*, 2093–2106.
- (23) Beaujuge, P. M.; Ellinger, S.; Reynolds, J. R. *Nat. Mater.* **2008**, *7*, 795–799.
- (24) Shi, P.; Amb, C. M.; Knott, E. P.; Thompson, E. J.; Liu, D. Y.; Mei, J.; Dyer, A. L.; Reynolds, J. R. *Adv. Mater.* **2010**, *22*, 4949–4953.
- (25) Blouin, N.; Michaud, A.; Gendron, D.; Wakim, S.; Blair, E.; Neagu-Plesu, R.; Belletête, M.; Durocher, G.; Tao, Y.; Leclerc, M. *J. Am. Chem. Soc.* **2008**, *130*, 732–742.
- (26) Chen, C.-H.; Hsieh, C.-H.; Dubosc, M.; Cheng, Y.-J.; Hsu, C.-S. *Macromolecules* **2010**, *43*, 697–708.
- (27) Peng, Q.; Park, K.; Lin, T.; Durstock, M.; Dai, L. *J. Phys. Chem. B* **2008**, *112*, 2801–2808.
- (28) Beaujuge, P. M.; Pisula, W.; Tsao, H. N.; Ellinger, S.; Müllen, K.; Reynolds, J. R. *J. Am. Chem. Soc.* **2009**, *131*, 7514–7515.
- (29) Kulkarni, A. P.; Zhu, Y.; Babel, A.; Wu, P.-T.; Jenekhe, S. A. *Chem. Mater.* **2008**, *20*, 4212–4223.
- (30) Salzner, U.; Karalti, O.; Durdađi, S. *J. Mol. Model.* **2006**, *12*, 687–701.
- (31) Salzner, U. *J. Phys. Chem. B* **2002**, *106*, 9214–9220.
- (32) Salzner, U.; Köse, M. E. *J. Phys. Chem. B* **2002**, *106*, 9221–9226.
- (33) Brzeziński, J. Z.; Reynolds, J. R. *Synthesis* **2002**, *2002*, 1053–1056.
- (34) Bijleveld, J. C.; Shahid, M.; Gilot, J.; Wienk, M. M.; Janssen, R. A. J. *Adv. Funct. Mater.* **2009**, *19*, 3262–3270.
- (35) Zhang, S.; Zhang, D.; Liebeskind, L. S. *J. Org. Chem.* **1997**, *62*, 2312–2313.
- (36) Hollinger, J.; Jahnke, A. A.; Coombs, N.; Seferos, D. S. *J. Am. Chem. Soc.* **2010**, *132*, 8546–8547.
- (37) Heeney, M.; Zhang, W.; Crouch, D. J.; Chabynyc, M. L.; Gordeyev, S.; Hamilton, R.; Higgins, S. J.; McCulloch, I.; Skabara, P. J.; Sparrowe, D.; Tierney, S. *Chem. Commun.* **2007**, 5061–5063.
- (38) Jahnke, A. A.; Howe, G. W.; Seferos, D. S. *Angew. Chem. Int. Ed.* **2010**, *49*, 10140–10144.
- (39) Ho, V.; Boudouris, B. W.; Segalman, R. A. *Macromolecules* **2010**, *43*, 7895–7899.
- (40) Yang, R.; Tian, R.; Yan, J.; Zhang, Y.; Yang, J.; Hou, Q.; Yang, W.; Zhang, C.; Cao, Y. *Macromolecules* **2005**, *38*, 244–253.
- (41) Cozzolino, A. F.; Britten, J. F.; Vargas-Baca, I. *Cryst. Growth Des.* **2006**, *6*, 181–186.
- (42) *CRC Handbook of Chemistry and Physics*, 92nd ed.; CRC Press: Boca Raton, FL, 2011.
- (43) Bauernschmitt, R.; Ahlrichs, R. *Chem. Phys. Lett.* **1996**, *256*, 454–464.
- (44) Frisch, M. J.; et al.; Gaussian, Inc.: Wallingford CT, 2009.
- (45) Becke, A. D. *J. Chem. Phys.* **1996**, *104*, 1040–1046.
- (46) Becke, A. D. *J. Chem. Phys.* **1993**, *98*, 5648–5652.
- (47) Yanai, T.; Tew, D.; Handy, N. *Chem. Phys. Lett.* **2004**, *393*, 51–57.
- (48) Hay, P. J.; Wadt, W. R. *J. Chem. Phys.* **1985**, *82*, 270.
- (49) Blouin, N.; Leclerc, M. *Acc. Chem. Res.* **2008**, *41*, 1110–1119.
- (50) Villar, H.; Otto, P.; Dupuis, M. *Synth. Met.* **1993**, *59*, 97–110.
- (51) Oyaizu, K.; Iwasaki, T.; Tsukahara, Y.; Tsuchida, E. *Macromolecules* **2004**, *37*, 1257–1270.
- (52) Jahnke, A. A.; Seferos, D. S. *Macromol. Rapid Commun.* **2011**, *32*, 943–951.
- (53) McCullough, R. *Adv. Mater.* **1998**, *10*, 93.
- (54) Kleinhenz, N.; Yang, L.; Zhou, H.; Price, S. C.; You, W. *Macromolecules* **2011**, *44*, 872–877.
- (55) Welch, G. C.; Coffin, R.; Peet, J.; Bazan, G. C. *J. Am. Chem. Soc.* **2009**, *131*, 10802–10803.
- (56) Welch, G. C.; Bazan, G. C. *J. Am. Chem. Soc.* **2011**, *133*, 4632–4644.